

# Unpaired Referring Expression Grounding via Bidirectional Cross-Modal Matching

Hengcan Shi, Munawar Hayat, Jianfei Cai

Monash University

{hengcan.shi, munawar.hayat, jianfei.cai}@monash.edu

## Abstract

Referring expression grounding is an important and challenging task in computer vision. To avoid the laborious annotation in conventional referring grounding, unpaired referring grounding is introduced, where the training data only contains a number of images and queries without correspondences. The few existing solutions to unpaired referring grounding are still preliminary, due to the challenges of learning image-text matching and lack of the top-down guidance with unpaired data. In this paper, we propose a novel bidirectional cross-modal matching (BiCM) framework to address these challenges. Particularly, we design a query-aware attention map (QAM) module that introduces top-down perspective via generating query-specific visual attention maps. A cross-modal object matching (COM) module is further introduced, which exploits the recently emerged image-text matching pretrained model, CLIP, to predict the target objects from a bottom-up perspective. The top-down and bottom-up predictions are then integrated via a similarity function (SF) module. We also propose a knowledge adaptation matching (KAM) module that leverages unpaired training data to adapt pre-trained knowledge to the target dataset and task. Experiments show that our framework outperforms previous works by 6.55% and 9.94% on two popular grounding datasets.

## 1 Introduction

Referring expression grounding aims to localize objects from an image based on a language query. It serves as a fundamental step for many higher-level multi-modal tasks, such as image captioning [Fan *et al.*, 2021], cross-modal retrieval [Yang *et al.*, 2021] and cross-modal segmentation [Shi *et al.*, 2020]. Most of previous methods are either fully-supervised [Zhang *et al.*, 2020; Suo *et al.*, 2021] or weakly-supervised [Gupta *et al.*, 2020; Liu *et al.*, 2021]. These methods require a mass of manually annotated bounding boxes and/or image-query pairs for training, as shown in Fig. 1 (a)&(b), which is laborious and needs human experts.

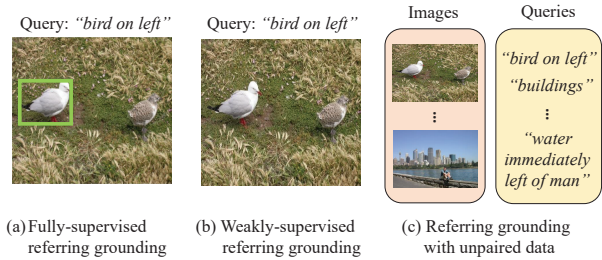


Figure 1: Examples of training data in different referring grounding scenarios. (a) Fully-supervised referring grounding that provides images, corresponding queries and bounding box annotations for training. (b) Weakly-supervised referring grounding which contains training images and corresponding queries. (c) Unpaired referring grounding which only includes a set of images and a number of queries.

To reduce the labor-intensive annotation, unpaired referring grounding has been attracting increasing research attention. The training set in this task only contains a number of images and some language queries, as depicted in Fig. 1 (c). In real-world applications, images and queries can be separately collected from web (e.g., public images from Google and object descriptions from Wikipedia) without manual annotations, or randomly generated using some language templates or automatic language generation tools with little human efforts. To correlate vision and language without paired training data, Wang *et al.* [Wang and Specia, 2019] leverage knowledge from pretrained object detection models, which simultaneously generate object proposals and their class names. They calculate similarities between class names and the query in the textual space to select the target object. Parcalabescu *et al.* [Parcalabescu and Frank, 2020] further use pretrained scene graph models to convert some visual context into language words to better calculate similarities with the query.

Despite significant progress made by these methods, a number of challenges remain unsolved. (1) There is a significant loss of information in the modality conversion in these methods. Either the class name or scene graph only contains limited features of objects, and critical clues such as color, position, posture, are not included in them. These features are very important for grounding, because queries often de-

scribe them. For example, in Fig. 1, it is hard to localize the “bird on left” by only using class names and scene graphs, since they do not contain the relative position information. (2) Meanwhile, these methods heavily rely on pre-extracted object proposals. They will not be able to find the desired object if it is not in the pre-extracted proposals. Moreover, object proposals can only provide local visual information, where global visual information is ignored. (3) These works only simply leverage knowledge from pretrained object detection models and scene graph generation models without any adaptation for the referring grounding task and the target data. Task and domain gaps between pre-learned knowledge and the target grounding dataset may decrease the accuracy.

On the other hand, a powerful image-text matching pre-trained model, called CLIP (contrastive language-image pre-training) [Radford *et al.*, 2021], has been introduced recently, which consists of an image encoder and a text encoder. It was trained on millions of image-caption pairs by a contrastive loss. Due to its good generalization ability, CLIP has been used as external knowledge in several applications, such as image generation [Jalal *et al.*, 2021] and image classification [Cheng *et al.*, 2021]. This motivates us to consider: *Can we exploit CLIP to address unpaired referring grounding problem?*

A straightforward way is to use CLIP image encoder to encode each proposal and CLIP text encoder to encode the query and then compare the encoded CLIP image and text directly. However, this only addresses the aforementioned first challenge since CLIP provides an aligned image-text embedding space. The other two challenges still remain. Therefore, in this paper, we propose a novel bidirectional cross-modal matching (BiCM) framework. In addition to the straightforward way of applying CLIP, which we call bottom-up matching handled by a cross-modal object matching (COM) module, we introduce a novel top-down matching branch, where we specifically designs a query-aware attention map (QAM) module that extracts query-specific attention maps based on the global image and query, and generates predictions from the attention maps to reduce the over-reliance on object proposals. A similarity fusion (SF) module is further designed to fuse the bottom-up and top-down matching results. We also propose a learnable knowledge adaptation matching (KAM) module, which adapts pretrained CLIP knowledge to the target grounding data and task. Extensive experiments on Flickr30K Entities [Plummer *et al.*, 2015] and ReferItGame [Kazemzadeh *et al.*, 2014] datasets demonstrate the effectiveness of our framework.

Our major contributions can be summarized as follows. (1) We propose a novel bidirectional cross-modal matching (BiCM) framework for unpaired referring grounding, where we design four components (QAM, COM, SF and KAM) to predict grounding results from both top-down and bottom-up perspectives and allow target-specific knowledge adaptation. (2) To the best of our knowledge, this is the first study to exploit CLIP knowledge for unpaired referring grounding. We explore CLIP feature space for cross-modal matching and propose a QAM module to extract query-aware visual attention maps from CLIP. (3) Extensive experimental results show that our proposed framework obtains significant

improvements on two popular referring grounding datasets.

## 2 Related Work

**Fully- and weakly-supervised referring grounding.** Fully-supervised referring grounding works [Hu *et al.*, 2016; Shi *et al.*, 2018; Qiu *et al.*, 2020; Mu *et al.*, 2021; Huang *et al.*, 2021] first use object detection models to extract a number of object proposals from the image. Then, cross-modal classifiers are trained to score each proposal based on its features and the language query features. Finally, the proposal with the highest score was chosen as the result. [Kamath *et al.*, 2021] uses Transformers to build end-to-end grounding. A major limitation of these methods is the required human annotation effort, which is very expensive (specially for large-scale datasets with massive language queries and bounding boxes). Weakly-supervised methods [Yeh *et al.*, 2018; Chen *et al.*, 2018; Gupta *et al.*, 2020; Liu *et al.*, 2021] do not need to annotate bounding boxes and only require image-query pairs. [Yeh *et al.*, 2018] leverages the image-query-pair training data to make co-occurrence statistics and predicts grounding results from these statistics. Other methods use cycle reconstruction [Chen *et al.*, 2018; Liu *et al.*, 2021] or contrastive learning [Gupta *et al.*, 2020] to allow weakly-supervised training. Although these works avoid bounding box annotations, they still need to label image-query pairs, which is also costly.

**Unpaired referring grounding.** Referring grounding with unpaired data is a promising learning paradigm to avoid manual annotations. In this task, there is neither image-query pairs nor bounding boxes in the training set. [Wang and Specia, 2019] uses object detection models trained on visual detection datasets to predict candidate bounding boxes and their class names. Next, it leverages textual datasets to train a text encoder and extracts features of the language query and box class names. Finally, it selects the desired bounding box by comparing each box class name features with the query features. [Parcalabescu and Frank, 2020] extracts context by pre-trained scene graph generation methods, which enriches the features of each box class name. However, these methods only simply employ pre-learned knowledge without any adaptation, and there are many information losses in modal conversions, which degrades their performance. In addition, they highly rely on pre-extracted proposals and class names.

## 3 Proposed Method

### 3.1 Problem Definition and Method Overview

The inputs of referring grounding are an image  $I$  and a language query  $Q$ . Referring grounding expects to output a bounding box  $P$  of the object described by the query. In this paper, we propose a bidirectional cross-modal matching (BiCM) framework to predict the bounding box. Our BiCM framework contains four components as shown in Fig. 2: (a) a query-aware attention map (QAM) module that generates attention maps and predicts a candidate bounding box in a top-down manner; (b) a cross-modal object matching (COM) module that leverages CLIP feature space to select bounding boxes from object proposals in a bottom-up manner; (c) a similarity fusion (SF) module that integrates the

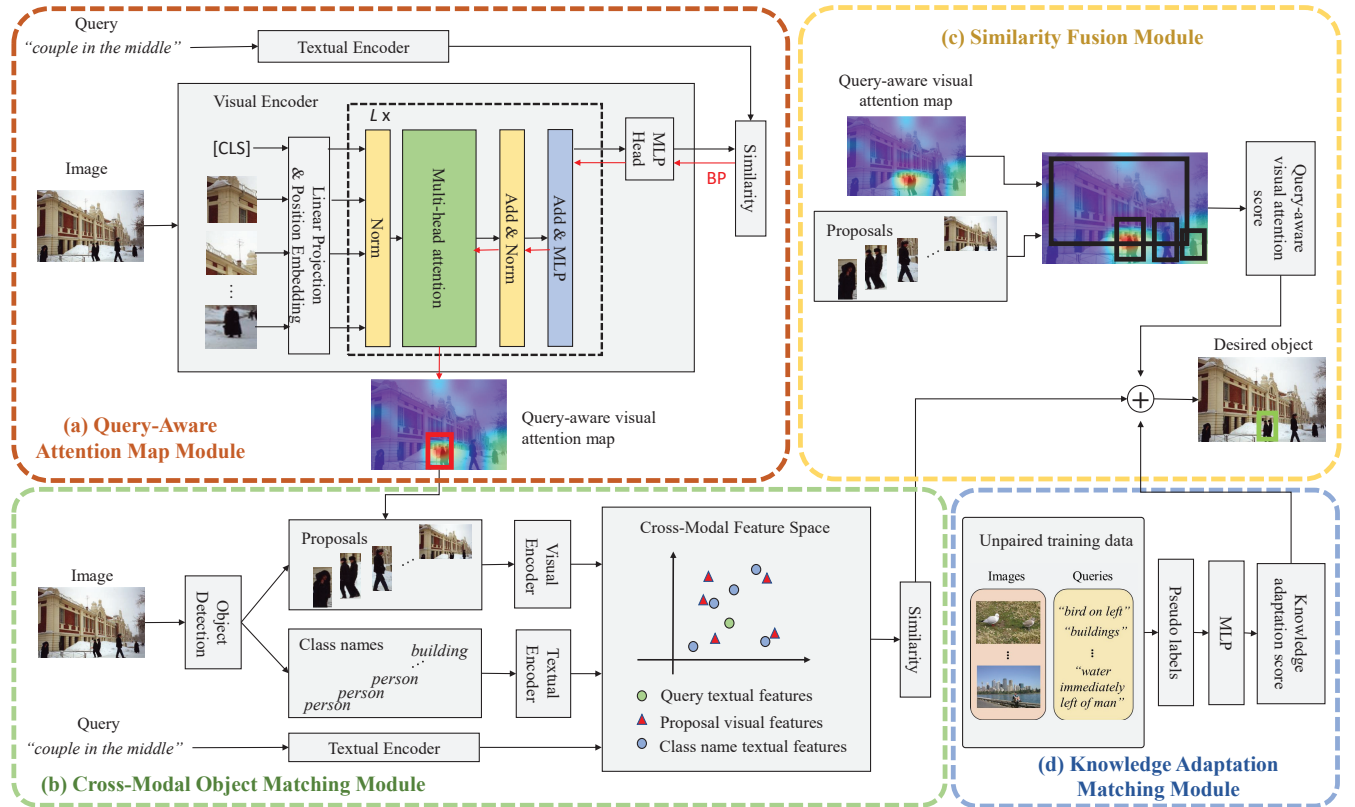


Figure 2: Illustration of BiCM. (a) A top-down QAM module extracts a query-aware visual attention map by back propagation (BP) and predicts a grounding result (the red box). (b) A bottom-up COM module selects the desired object from object proposals. The result from QAM is added, to avoid the over-reliance on pre-extracted proposals. (c) An SF module fuses the predictions from QAM and COM. (d) A KAM module leverages unpaired training data to adapt pretrained knowledge to the target grounding dataset to further improve the accuracy.

top-down and bottom-up results; (d) and a knowledge adaptation matching (KAM) module that adapts CLIP knowledge to our target grounding data. We introduce the details of each component below.

### 3.2 Query-Aware Attention Map Module

The top-down QAM module aims to generate the grounding result from the global image and query. Inspired by Grad-CAM [Selvaraju *et al.*, 2017] in CNN, we design a back-propagation-based mechanism to extract query-aware visual attention maps in Transformers to achieve this goal.

As shown in Fig. 2 (a), we first input the image  $I$  into the pre-trained CLIP visual encoder (ViT [Dosovitskiy *et al.*, 2020]) and output the feature vector  $\mathbf{f}_i$ . In ViT, the input image is divided into  $U$  patches (tokens) and a special [CLS] token is added to generate  $\mathbf{f}_i$ . Visual attention is extracted from the last block in ViT as follows:

$$att_{h,u} = \text{Softmax}\left(\frac{\mathbf{q}_h \mathbf{k}_{h,u}^T}{\sqrt{d}}\right) \quad (1)$$

where  $h = 1, \dots, H$  and  $H$  is the number of heads in the last block.  $\mathbf{q}_h$  is the attention “query” of the [CLS] token in the  $h$ -th head, and  $\mathbf{k}_{h,u}$  represents the attention “key” of the  $u$ -th image patch.  $d$  is a scaling factor.  $att_{h,u}$  is the attention score of the  $u$ -th image patch in the  $h$ -th head, which means

the importance of this image patch for the final output. It can be used to highlight visually salient regions in the image. However, this attention score cannot find out the regions corresponding to the language query  $Q$ .

To generate query-aware attention scores, we leverage the pre-trained CLIP textual encoder (GPT-2 [Radford *et al.*, 2019]) to encode the feature vector  $\mathbf{f}_q$  of the input query  $Q$ . Since the image feature vector  $\mathbf{f}_i$  and the query feature vector  $\mathbf{f}_q$  are embedded into the same feature space, we calculate their cosine similarity  $S^{IQ}$  as

$$S^{IQ} = \frac{\langle \mathbf{f}_i, \mathbf{f}_q \rangle}{\|\mathbf{f}_i\| \|\mathbf{f}_q\|} \quad (2)$$

where  $\langle \cdot, \cdot \rangle$  represents inner product.

We then take the image-query similarity  $S^{IQ}$  as a loss and propagate it back into the visual encoder:

$$\alpha_{h,u} = \frac{\partial S^{IQ}}{\partial att_{h,u}} \quad (3)$$

where  $\alpha_{h,u}$  is the gradient on  $att_{h,u}$ , which can be regarded as the importance of this attention score for the image-query similarity  $S^{IQ}$ . Thus, we use it to weight the attention score to find out the most important image patches for the language query as

$$\tilde{att}_{h,u} = att_{h,u} \times \text{ReLU}(\alpha_{h,u}) \quad (4)$$

where  $\widetilde{att}_{h,u}$  is the weighted attention score, and ReLU function is used to filter out the negative importance scores. We average scores in all heads as our final query-aware visual attention score  $qa_u$ :

$$a_u = \frac{1}{H} \sum_{h=1}^H \widetilde{att}_{h,u}. \quad (5)$$

Scores  $a_u$  for all image patches construct a query-aware visual attention map  $A$ . We finally upsample  $A$  into the original image size by bilinear interpolation and use min-max normalization to normalize it. By empirically setting a threshold  $Thr_a$ , we can select out the desired object and generate the bounding box  $P_t$ .

### 3.3 Cross-Modal Object Matching Module

Our QAM module is able to localize objects from the top-down perspective. Nevertheless, it cannot always capture compact object boundaries. Thus, we further introduce a bottom-up method to identify objects from pre-extracted object proposals.

In particular, an object detection model such as Faster RCNN [Ren *et al.*, 2015] is first used to generate object proposals  $\{P_r\}_{r=1}^{N_r}$  from the input image  $I$ , where  $N_r$  denotes the number of proposals in the image. Then, we leverage the CLIP visual encoder to extract visual feature vector  $\mathbf{fp}_r$  of each proposal. After that, we compute the similarity  $S_r^{PQ}$  between the query and each proposal as

$$S_r^{PQ} = \frac{\langle \mathbf{fp}_r, \mathbf{fq} \rangle}{\|\mathbf{fp}_r\| \|\mathbf{fq}\|}. \quad (6)$$

This similarity directly compares the visual features of objects with the language query, and thus avoids information loss caused by modality conversion.

In addition, previous works [Wang and Specia, 2019; Parcalabescu and Frank, 2020] indicate that class names of object proposals are also important information. Therefore, we further calculate the similarity between the query  $Q$  and each proposal class name  $C_r$ . We use the CLIP textual encoder to encode  $C_r$  into the feature vector  $\mathbf{fc}_r$  and then compute the cosine similarity:

$$S_r^{CQ} = \frac{\langle \mathbf{fc}_r, \mathbf{fq} \rangle}{\|\mathbf{fc}_r\| \|\mathbf{fq}\|} \quad (7)$$

The final bottom-up similarity  $S_r^{BU}$  between each proposal and the query is defined as the sum of the two similarities:

$$S_r^{BU} = S_r^{PQ} + S_r^{CQ}. \quad (8)$$

The proposal  $P_r$  with the highest similarity could be selected as the desired object.

Benefiting from the pretrained object detection model, our bottom-up COM module can extract compact object boundaries. However, it cannot predict the desired object if the pretrained detection model misses the object. To avoid this, we add our top-down prediction  $P_t$  to the set of object proposals  $\{P_r\}_{r=1}^{N_r}$  and select the desired object from the combined set  $\{P_1, \dots, P_{N_r}, P_t\}$ . We take the proposal class name  $C_r$  which has the highest similarity  $S_r^{CQ}$  with the query as the class name of  $P_t$ .

### 3.4 Similarity Fusion Module

The SF module is to integrate the similarity scores from the top-down QAM module and the bottom-up COM module, as shown in Fig. 2 (c). For each object proposal in  $\{P_1, \dots, P_R, P_t\}$ , we generate its top-down similarity based on the query-aware visual attention map  $A$  as

$$S_r^{TD} = \frac{1}{N_v} \sum_{v=1}^{N_v} a_v \quad (9)$$

where  $N_v$  is the number of pixels in this proposal and  $a_v$  is the attention score of each pixel  $v$  in  $A$ .

We then fuse the top-down and bottom-up scores as follows:

$$S_r = S_r^{BU} + \lambda_t S_r^{TD} \quad (10)$$

where  $\lambda_t$  is the weight to trade off the two scores. The final result is the proposal whose fused score is the highest.

### 3.5 Knowledge Adaptation Matching Module

The purpose of this KAM module is to generate pseudo labels from unpaired training data and train a lightweight network to adapt CLIP knowledge to the target dataset and the grounding task. Specifically, given the unpaired image and query sets, we leverage CLIP visual and textual encoders to obtain the image and query features, respectively. For each image, we find out the query with the highest similarity, and treat the image and the query as a pseudo image-query pair. Then, for each image-query pair, we use the above three components to predict a bounding box. If its fused similarity score  $S_r$  is higher than a threshold  $Thr_k$ , we choose the bounding box as a pseudo label or pseudo ground-truth.

After constructing pseudo labels, we then train a simple MLP (Multi-layer Perception) network, which takes the image features  $\mathbf{fi}$ , visual object proposal features  $\mathbf{fp}_r$ , object class name features  $\mathbf{fc}_r$  and query features  $\mathbf{fq}$  as inputs, and outputs another similarity score  $S_r^{KAM}$ . We adopt the loss in fully-supervised grounding [Hu *et al.*, 2016] to train the MLP. During inference, the score  $S_r^{KAM}$  can be added to  $S_r$  to select the target object:

$$Sim_r = S_r^{BU} + \lambda_t S_r^{TD} + \lambda_k S_r^{KAM} \quad (11)$$

where  $\lambda_k$  is the weight of  $S_r^{KAM}$ .

## 4 Experiments

### 4.1 Experimental Setting

**Datasets.** We evaluate our method on the Flickr30K Entities [Plummer *et al.*, 2015] and ReferItGame [Kazemzadeh *et al.*, 2014] datasets. The Flickr30K Entities dataset [Plummer *et al.*, 2015] consists of 31783 images, 513644 queries and 275775 bounding boxes. Many queries (e.g., *several people*) describe multiple bounding boxes in an image. In this case, following previous methods [Wang and Specia, 2019; Parcalabescu and Frank, 2020], we merge these bounding boxes and use the union region as the ground truth. This dataset is split into training, validation and testing sets, containing 29783, 1000 and 1000 images, respectively. The ReferItGame dataset [Kazemzadeh *et al.*, 2014], also known

as RefCLEF, contains 20000 images, 9000 for training, 1000 for validation and 10000 for testing. 130525 queries describe 96654 objects in these images. On both two datasets, we extract pseudo labels from unpaired data in the training and validation sets, and evaluate our method on the testing sets.

**Metrics.** We adapt the grounding accuracy to estimate our grounding framework, which is percentage of predictions whose IoU with ground truth is higher than 0.5.

**Implementation Details.** We use Faster RCNN [Ren *et al.*, 2015] pretrained on Visual Genome [Krishna *et al.*, 2017] to extract 100 object proposals for each image, and encode 512-dimension visual and textual features. Thresholds  $Thr_a$  and  $Thr_k$  are set to 0.7 and 0.9, respectively. We set  $\lambda_t$  and  $\lambda_k$  to 1000 and 1, to make the three scores have similar orders of magnitude. Our MLP is trained on one Nvidia RTX 3090 GPU for 50 epochs. Adam optimizer is used for training and the base learning rate is set to 0.0001. On the Flickr30K Entities dataset, because some queries refer to multiple bounding boxes in an image, all methods including ours merge multiple high-score bounding boxes as final results. We merge bounding boxes whose similarities are higher than the average similarity. On the ReferItGame dataset, a query only describes one object in an image. To fairly compared with previous work [Wang and Specia, 2019], we select the largest bounding box from above-average-similarity bounding boxes as our prediction.

## 4.2 Quantitative Results

Table 1 shows results of our and other state-of-the-art methods on the Flickr30K Entities dataset. For a fair comparison, all unpaired-data methods use Faster RCNN pretrained on Visual Genome [Krishna *et al.*, 2017] to extract proposals. Moreover, in [Parcalabescu and Frank, 2020], results of [Wang and Specia, 2019] and [Parcalabescu and Frank, 2020] on a non-standard testing set with 16,576 phrases are reported. We reproduce these methods on the standard testing set with 14,481 queries. Compared with [Wang and Specia, 2019] which only uses class name information, our method achieves improvements by 8.21%. [Parcalabescu and Frank, 2020] employs scene graphs to improve referring grounding in their method. Our method outperforms their method by 6.55%.

Results on the ReferItGame dataset are shown in Table 2. It can be observed that our method outperforms [Wang and Specia, 2019] and [Parcalabescu and Frank, 2020] by 12.46% and 9.94%, respectively. These results demonstrate the effectiveness of our BiCM framework.

In Table 1 and Table 2, we report results from some fully- and weakly-supervised methods as references. Our method and previous unpaired methods [Wang and Specia, 2019; Parcalabescu and Frank, 2020] outperform many weakly-supervised methods. A reason is that we introduce external knowledge. Our method also shows competitive accuracy against some fully-supervised methods, such as [Dogan *et al.*, 2019] and [Plummer *et al.*, 2017].

## 4.3 Ablation Studies

**Effects of main components.** We first study the effects of each main component in our framework (see Table 3). Com-

Method	Accuracy (%)
<i>Fully-supervised</i>	
[Rohrbach <i>et al.</i> , 2016]	47.81
[Plummer <i>et al.</i> , 2017]	55.85
[Dogan <i>et al.</i> , 2019]	61.60
[Yang <i>et al.</i> , 2020]	69.53
[Mu <i>et al.</i> , 2021]	<b>78.73</b>
<i>Weakly-supervised</i>	
[Rohrbach <i>et al.</i> , 2016]	28.94
[Yeh <i>et al.</i> , 2018]	36.93
[Gupta <i>et al.</i> , 2020]	51.67
[Liu <i>et al.</i> , 2021]	<b>59.27</b>
<i>Unpaired Data</i>	
[Wang and Specia, 2019]	53.25
[Wang and Specia, 2019]*	56.30
[Parcalabescu and Frank, 2020]	54.91
[Parcalabescu and Frank, 2020]*	57.08
Ours	<b>61.46</b>

Table 1: Grounding accuracy on the Flickr30K Entities test. “\*” means results estimated on a non-standard testing set with 16,576 queries.

Method	Accuracy (%)
<i>Fully-supervised</i>	
[Rohrbach <i>et al.</i> , 2016]	26.93
[Plummer <i>et al.</i> , 2018]	34.15
[Bajaj <i>et al.</i> , 2019]	44.91
[Mu <i>et al.</i> , 2021]	65.15
[Huang <i>et al.</i> , 2021]	<b>67.47</b>
<i>Weakly-supervised</i>	
[Chen <i>et al.</i> , 2018]	15.83
[Yeh <i>et al.</i> , 2018]	20.91
[Liu <i>et al.</i> , 2019]	26.19
[Liu <i>et al.</i> , 2021]	<b>37.68</b>
<i>Unpaired Data</i>	
[Wang and Specia, 2019]	27.56
[Parcalabescu and Frank, 2020]	30.08
Ours	<b>40.02</b>

Table 2: Grounding accuracy on the ReferItGame test.

pared with the baseline method, our COM module yields 4.35% improvements, because COM directly analyzes multi-modal data and thus avoids information loss during modality conversion. The performance of our QAM module is lower than the baseline. The reason is that our QAM can localize objects from a top-down perspective but cannot always capture accurate object boundaries. However, when we add the bounding box generated by QAM to COM (i.e., QAM+COM), we achieve higher accuracy than both the baseline and original COM, indicating that our top-down QAM and bottom-up COM are complementary. QAM can find objects which are missed in pre-extracted proposals in COM, while COM is able to select bounding boxes with better boundaries. Our SF module further fuses the top-down query-aware visual attention maps with bottom-up similarity scores, and thus improves the accuracy by 1.72%. The learnable KAM module achieves improvements of 1.31%, thanks to the knowledge adaptation.

**BiCM with or without training.** The QAM, COM and SF modules in our BiCM do not need any training. Com-

Method	Accuracy (%)
Baseline [Wang and Specia, 2019]	53.25
QAM	30.86
COM	57.60
QAM+COM	58.43
QAM+COM+SF	60.15
QAM+COM+SF+KAM	61.46

Table 3: The effects of the main components on Flickr30K Entities test.

Method	Accuracy (%)
COM	57.60
QAM (VA) + COM	57.85
QAM (QA) + COM	58.43
QAM (VA) + COM + SF	57.97
QAM (QA) + COM + SF	60.15

Table 4: The effects of different top-down maps on Flickr30K Entities test. “VA” means visual attention maps, while “QA” means our query-aware visual attention maps.

pared with the baseline, our method without training yields 6.90% improvements. Our KAM module extracts pseudo labels from unpaired training data to train an MLP. Our method with KAM outperforms the baseline by 8.21%.

**Different attention maps in the top-down module.** We show the effects of our query-aware visual attention maps in Table 4. Vanilla visual attention maps are composed by attention scores  $\{att_{h,u}\}_{u=1}^U$ , which is able to highlight visually salient regions but cannot highlight regions corresponding to the language query. Therefore, it only slightly improves the performance, compared with only using COM. Our query-aware visual attention maps find out not only visual salient regions but also query-specific regions, as shown in Fig. 3. Thus, our query-aware visual attention maps achieve significant improvements.

**Different information in the bottom-up module.** Table 5 shows the effects of different information in our COM module. When COM only uses object class names, the performance is higher than the baseline. This is because our textual encoder models the information of the entire query while the baseline method only separately models information of every words. Compared with using object class names, using object visual information shows a lower accuracy. A reason is that class names and queries are in the same modality while visual information and queries are in different modalities. Even though our COM embeds information in different modalities into a same space, comparing single-modal information is still easier than comparing multi-modal information. In addition, many queries only contain one word or several words, which are very similar to class names. Therefore, using class names shows better performance. However, leveraging both class names and visual information obtains the best performance and gains significant improvements (3.51%) compared with using only a single modality. It is because class names lack some important information such as color, posture and so on, which can be provided by vision.

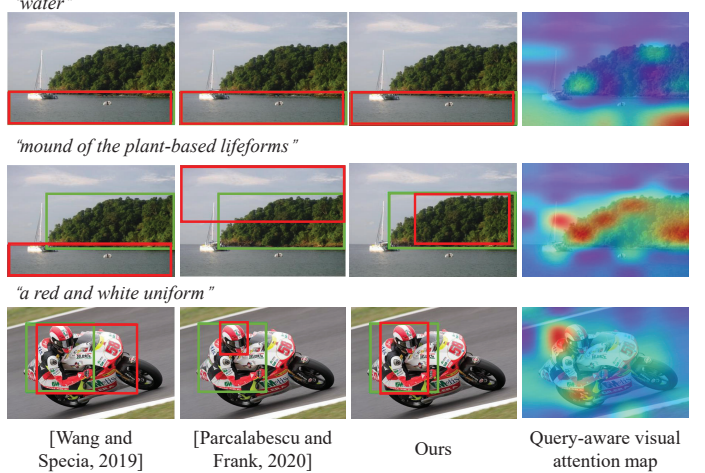


Figure 3: Grounding results of different methods, and our query-aware visual attention maps on ReferItGame test set (the first and second rows) and the Flickr30K Entities test set (the third row). Red boxes denote predictions and green boxes are ground truths.

Information	Accuracy (%)
Baseline [Wang and Specia, 2019]	53.25
object class name	54.09
visual object	40.29
visual object + class name	57.60

Table 5: The effects of different bottom-up information settings on Flickr30K Entities test. We only use COM in this experiment.

#### 4.4 Qualitative Results

We visualize some grounding results in Fig. 3. It is seen that while previous methods do well at finding objects when the query is a noun (the first row in Fig. 3), they mis-localize many objects for relatively complex queries (e.g., the second and third rows in Fig. 3). The reason is that previous technologies only use class names and scene graphs to compare with queries, while some key information described in these queries are not contained in object class names, such as color and position. Different from previous methods, our method leverages bidirectional matching and knowledge adaptation, and thus avoids these grounding errors.

#### 5 Conclusion

In this paper, we have presented a BiCM framework for unpaired referring grounding. It includes four major components: a top-down QAM module to extract query-aware attention maps, a bottom-up COM module to directly compare multi-modal information, an SF module to integrate top-down and bottom-up results, and a KAM module that leverages pseudo training data to adapt external knowledge to the target grounding data. Experimental results have demonstrated that our proposed method outperforms the existing state-of-the-art methods by a large margin on two popular referring grounding datasets.

## References

[Bajaj *et al.*, 2019] Mohit Bajaj, Lanjun Wang, and Leonid Sigal. G3raphground: Graph-based language grounding. In *ICCV*, 2019.

[Chen *et al.*, 2018] Kan Chen, Jiyang Gao, and Ram Nevatia. Knowledge aided consistency for weakly supervised phrase grounding. In *CVPR*, 2018.

[Cheng *et al.*, 2021] Ruizhe Cheng, Bichen Wu, et al. Data-efficient language-supervised zero-shot learning with self-distillation. In *CVPR*, 2021.

[Dogan *et al.*, 2019] Pelin Dogan, Leonid Sigal, et al. Neural sequential phrase grounding (seqground). In *CVPR*, 2019.

[Dosovitskiy *et al.*, 2020] Alexey Dosovitskiy, Lucas Beyer, et al. An image is worth 16x16 words: Transformers for image recognition at scale. *arXiv preprint arXiv:2010.11929*, 2020.

[Fan *et al.*, 2021] Zhihao Fan, Zhongyu Wei, et al. Tcic: Theme concepts learning cross language and vision for image captioning. *IJCAI*, 2021.

[Gupta *et al.*, 2020] Tanmay Gupta, Arash Vahdat, et al. Contrastive learning for weakly supervised phrase grounding. *ECCV*, 2020.

[Hu *et al.*, 2016] Ronghang Hu, Huazhe Xu, et al. Natural language object retrieval. In *CVPR*, 2016.

[Huang *et al.*, 2021] Binbin Huang, Dongze Lian, et al. Look before you leap: Learning landmark features for one-stage visual grounding. In *CVPR*, 2021.

[Jalal *et al.*, 2021] Ajil Jalal, Sushrut Karmalkar, et al. Fairness for image generation with uncertain sensitive attributes. In *ICML*, 2021.

[Kamath *et al.*, 2021] Aishwarya Kamath, Mannat Singh, et al. Mdetr-modulated detection for end-to-end multimodal understanding. In *ICCV*, 2021.

[Kazemzadeh *et al.*, 2014] Sahar Kazemzadeh, Vicente Ordonez, et al. Referitgame: Referring to objects in photographs of natural scenes. In *EMNLP*, 2014.

[Krishna *et al.*, 2017] Ranjay Krishna, Yuke Zhu, et al. Visual genome: Connecting language and vision using crowdsourced dense image annotations. *IJCV*, 2017.

[Liu *et al.*, 2019] Xuejing Liu, Liang Li, et al. Adaptive reconstruction network for weakly supervised referring expression grounding. In *ICCV*, 2019.

[Liu *et al.*, 2021] Yongfei Liu, Bo Wan, et al. Relation-aware instance refinement for weakly supervised visual grounding. In *CVPR*, 2021.

[Mu *et al.*, 2021] Zongshen Mu, Siliang Tang, et al. Disentangled motif-aware graph learning for phrase grounding. In *AAAI*, 2021.

[Parcalabescu and Frank, 2020] Letitia Parcalabescu and Anette Frank. Exploring phrase grounding without training: Contextualisation and extension to text-based image retrieval. In *CVPR*, 2020.

[Plummer *et al.*, 2015] Bryan A Plummer, Liwei Wang, et al. Flickr30k entities: Collecting region-to-phrase correspondences for richer image-to-sentence models. In *ICCV*, 2015.

[Plummer *et al.*, 2017] Bryan A Plummer, Arun Mallya, et al. Phrase localization and visual relationship detection with comprehensive image-language cues. In *ICCV*, 2017.

[Plummer *et al.*, 2018] Bryan A Plummer, Paige Kordas, et al. Conditional image-text embedding networks. In *ECCV*, 2018.

[Qiu *et al.*, 2020] Heqian Qiu, Hongliang Li, et al. Language-aware fine-grained object representation for referring expression comprehension. In *ACMMM*, 2020.

[Radford *et al.*, 2019] Alec Radford, Jeffrey Wu, et al. Language models are unsupervised multitask learners. *OpenAI blog*, 1(8):9, 2019.

[Radford *et al.*, 2021] Alec Radford, Jong Wook Kim, et al. Learning transferable visual models from natural language supervision. *arXiv preprint arXiv:2103.00020*, 2021.

[Ren *et al.*, 2015] Shaoqing Ren, Kaiming He, et al. Faster r-cnn: Towards real-time object detection with region proposal networks. In *NeurIPS*, 2015.

[Rohrbach *et al.*, 2016] Anna Rohrbach, Marcus Rohrbach, et al. Grounding of textual phrases in images by reconstruction. In *ECCV*, 2016.

[Selvaraju *et al.*, 2017] Ramprasaath R Selvaraju, Michael Cogswell, et al. Grad-cam: Visual explanations from deep networks via gradient-based localization. In *ICCV*, 2017.

[Shi *et al.*, 2018] Hengcan Shi, Hongliang Li, et al. Keyword-aware network for referring expression image segmentation. In *ECCV*, 2018.

[Shi *et al.*, 2020] Hengcan Shi, Hongliang Li, et al. Query reconstruction network for referring expression image segmentation. *TMM*, 2020.

[Suo *et al.*, 2021] Wei Suo, Mengyang Sun, et al. Proposal-free one-stage referring expression via grid-word cross-attention. *IJCAI*, 2021.

[Wang and Specia, 2019] Josiah Wang and Lucia Specia. Phrase localization without paired training examples. In *ICCV*, 2019.

[Yang *et al.*, 2020] Sibei Yang, Guanbin Li, and Yizhou Yu. Propagating over phrase relations for one-stage visual grounding. In *ECCV*, 2020.

[Yang *et al.*, 2021] Yang Yang, Chubing Zhang, et al. Rethinking label-wise cross-modal retrieval from a semantic sharing perspective. *IJCAI*, 2021.

[Yeh *et al.*, 2018] Raymond A Yeh, Minh N Do, et al. Unsupervised textual grounding: Linking words to image concepts. In *CVPR*, 2018.

[Zhang *et al.*, 2020] Zhu Zhang, Zhou Zhao, et al. Object-aware multi-branch relation networks for spatio-temporal video grounding. *IJCAI*, 2020.

## A Visualization of Query-Aware Visual Attention Map

We visualize our query-aware visual attention map in Fig. 4. It can be seen that vanilla visual attention maps only find out visually salient regions (such as the tower in the first image in Fig. 4), while our query-aware maps highlight objects corresponding to different language queries.

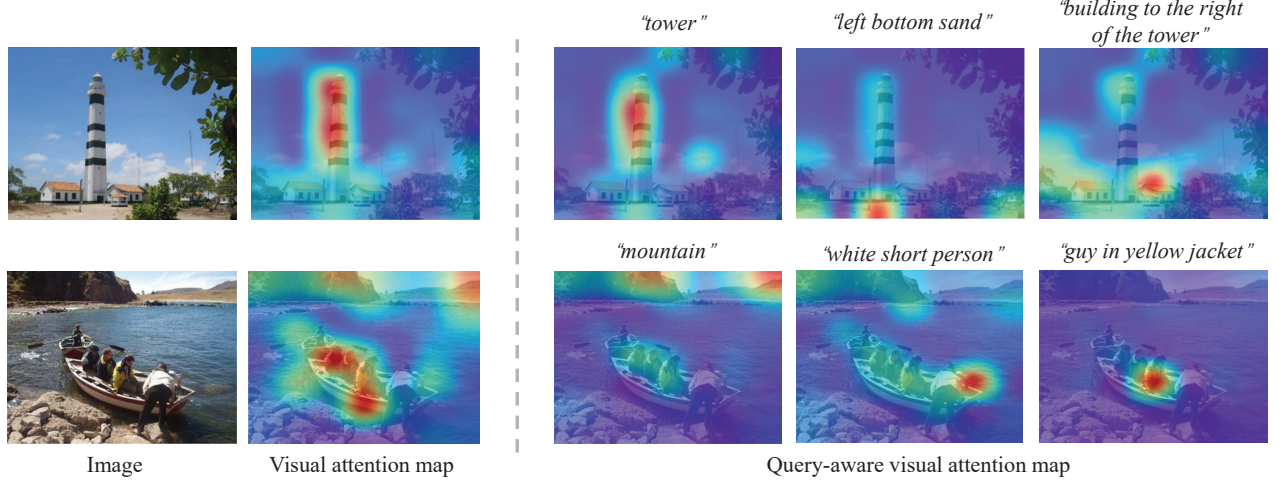


Figure 4: Comparison of visual attention map and our proposed query-aware visual attention map on the ReferItGame dataset.

## B Visualization of Grounding Results

Fig. 5 shows more qualitative grounding results on the Flickr30K Entities and ReferItGame datasets. Compared with previous methods [Wang and Specia, 2019; Parcalabescu and Frank, 2020], our method finds out the desired objects more accurately.



Figure 5: Grounding results on Flickr30K Entities test (left three columns) and ReferItGame test (right three columns). Red boxes denote predictions while green boxes are ground truths.

## C MLP in Knowledge Adaptation Matching Module

Our MLP in KAM consists of three fully-connected layers with batch normalization and ReLU activation. The first layer is used to fuse input features, the second layer is to transform the fused features and the final layer outputs the score  $S_r^{KAM}$  which is normalized by a Sigmoid function.

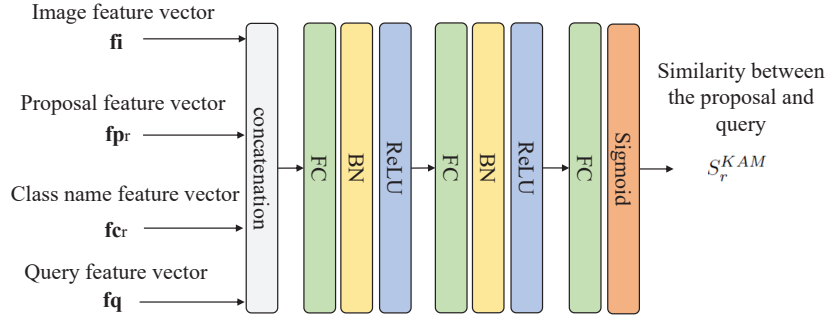


Figure 6: Illustration of the MLP in KAM. “FC” means the fully connected layer. “BN” represents the batch normalization layer. “ReLU” and “Sigmoid” are ReLU activation and Sigmoid normalization, respectively.

## D Precision of Pseudo Labels

To train the MLP in KAM, we extract pseudo labels from unpaired training data. Table 6 shows the precision of our pseudo labels, which is the percentage of correct ones in all pseudo labels we extracted. It can be observed that our precision is 74.7% when the threshold  $Thr_k$  is 0.9. Under this threshold, we can generate 3,986 pseudo annotations.

$Thr_k$	Number of pseudo labels	Precision (%)
0.6	6058	64.2
0.7	5180	68.5
0.8	4401	70.4
0.9	3986	74.7

Table 6: The effects of different pseudo label thresholds  $Thr_k$  on Flickr30K Entities trainval.

## E Failure Cases

We depict some failure cases in Fig. 7. There are two main types of failures. The first is caused by complex reasoning. For instance, in the left two images in Fig. 7, the queries require counting and analyzing numbers, which is hard to be learned by unpaired training data. The second type is inaccurate object boundary, such as the right two images in Fig. 7. Our BiCM finds out the desired objects but sometimes fails to capture their boundaries. Using better object detection models can reduce this type of errors.

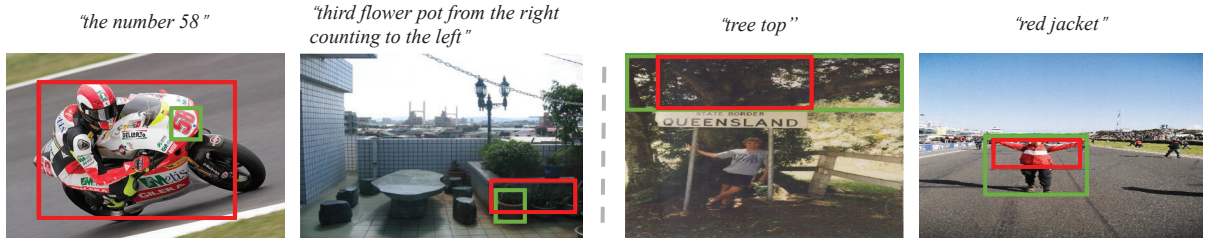


Figure 7: Failure cases of our method. Red and green boxes are grounding results and ground truths, respectively.